Please note that this is a postprint version.
The final version published in Pain (vol. 142, issue 3, pages 225-235) is available at: http://journals.lww.com/pain/Abstract/2009/04000/Involvement_of_voltage_gated_sodium_channels.12.aspx
or upon request to the corresponding author at jeanfrancois.desaphy@ubina.it

Involvement of voltage-gated sodium channels blockade in the analgesic effects of orphenadrine.

Jean-François Desaphy [a,1,*], Antonella Dipalma [a,1], Michela De Bellis [a], Teresa Costanza [a], Christelle Gaudioso [b], Patrick Delmas [b], Alfred L. George Jr. [c], Diana Conte Camerino [a]

[a] *Sezione di Farmacologia, Dipartimento FarmacoBiologico, Facoltà di Farmacia, Università di Bari, Bari, Italy*
[b] *CRN2M, CNRS UMR 6231, Université de la Méditerranée, CS80011.Bd Pierre Dramard, 13344 Marseille Cedex 15, France*
[c] *Division of Genetic Medicine, Department of Medicine, Vanderbilt University, 529 Light Hall, Nashville, TN 37232-0275, USA*

*** Corresponding author. Address: Sezione di Farmacologia, Dipartimento FarmacoBiologico, via Orabona 4-campus, 70125 Bari, Italy. Tel.: +39 080 544 27 61; fax: +39 080 544 28 01.**
E-mail address: **jfdesaphy@farmbiol.uniba.it (J.-F. Desaphy)**
[1] These authors contributed equally to this article

Abstract

Orphenadrine is a drug acting on multiple targets, including muscarinic, histaminic, and NMDA receptors. It is used in the treatment of Parkinson's Disease and in musculoskeletal disorders. It is also used as an analgesic, although its mechanism of action is still unknown. Physiological and pharmacological results both have demonstrated a critical role for voltage-gated sodium channels in many types of chronic pain syndromes. We tested the hypothesis that orphenadrine may block voltage-gated sodium channels. By using patch-clamp, we evaluated the effects of the drug on whole-cell sodium currents in HEK293 cells expressing the skeletal muscle (Nav1.4), cardiac (Nav1.5) and neuronal (Nav1.1 and Nav1.7) subtypes of human sodium channels, as well as on whole-cell tetrodotoxin (TTX)-resistant sodium currents likely conducted by Nav1.8 and Nav1.9 channel subtypes in primary culture of rat DRG sensory neurons. The results indicate that orphenadrine inhibits sodium channels in a concentration, voltage and frequency dependent manner. Using site-directed mutagenesis, we further show that orphenadrine binds to the same receptor as the local anesthetics. Orphenadrine affinities for resting and inactivated sodium channels were higher compared to those of known sodium channels blockers, such as mexiletine and flecainide. Low, clinically-relevant orphenadrine concentration produces significant block of Nav1.7, Nav1.8, and Nav1.9 channels, which are critical for experiencing pain sensations, indicating a role for sodium channel blockade in the clinical efficacy of orphenadrine as analgesic compound. On an other hand, block of Nav1.1 and Nav1.5 may contribute to the proconvulsive and proarrhythmic adverse reactions, especially observed during overdose.

1. Introduction

Orphenadrine is an anticholinergic agent used mainly in the treatment of Parkinson's disease to alleviate some of the troublesome symptoms of the disease, especially the involuntary resting tremor [44,45]. In addition to this use, the drug has a long history in the clinics as a muscle relaxant [19]. The mechanism of action for such effect remains unclear, but may be related in part to sedative effects; orphenadrine exerts unspecific antagonist activity at the phencyclidine binding site of N-methyl-D-aspartate (NMDA) receptors, one of the subtypes of glutamate receptors [24]. A study reported that orphenadrine is able to protect cultured cerebellar neurons from excitotoxicity following direct exposure of neurons [17].

Orphenadrine is used also as an analgesic both alone or in association with non steroidal anti-inflammatory drugs [21]. In a human model of capsaicin-dependent inflammatory pain obtained with laser somatosensory evoked potentials, orphenadrine citrate was able to exert an analgesic/anti-hyperalgesic effect in a low-dose (30 mg/day), which was predominantly due to central/spinal mechanisms [42]. A central action of orphenadrine was thus proposed, but the detailed mechanisms are unknown.

Orphenadrine is a monomethylated derivative of diphenydramine, an antihistaminic drug. Since histamine plays an important role in pain processes, it is possible that the analgesic action of orphenadrine may be related to histamine antagonism. However, diphenydramine was also shown to block voltage-gated sodium channels [22], suggesting that other pharmacologic properties may contribute to antinociceptive effects of orphenadrine. Physiological and pharmacological evidence both have demonstrated a critical role for voltage-gated sodium channels in many types of chronic pain syndromes, because these channels play a fundamental role in the excitability of neurons in the central and peripheral nervous systems [10]. Recent findings strengthen this view, since a gain of function of the Nav1.7 channel, expressed at high levels in nociceptive dorsal root ganglion (DRG) neurons, was shown to cause primary erythermalgia and paroxysmal extreme pain disorder, two inherited pain syndromes linked to SCN9A mutations and responsive to lidocaine, mexiletine and carbamazepine treatment [15, 30, 49]. Conversely, loss of function of Nav1.7 channels results in an inherited channelopathy characterized by total insensitivity to pain of any type [9]. Moreover, expression levels of the Nav1.3 channel isoform increase in DRG following neuronal injury or an inflammatory insult [3]. Finally, knocking-out the Nav1.8 or Nav1.9 channel isoforms in mice has been shown to cause deficits in thermal and mechanical pain perception [1, 7, 35].

In the current study, we tested the hypothesis that orphenadrine may block voltage-gated sodium channels. We evaluated the effects of the drug on muscle, cardiac and neuronal human subtypes of sodium channels heterologously expressed in HEK293 cells and elucidated the molecular mechanism of block by orphenadrine by using specific voltage-clamp protocols and sodium channel site-directed mutagenesis. We also tested orphenadrine on tetrodotoxin (TTX)-resistant sodium currents in sensory neurons dissociated from rat dorsal root ganglions (DRG). A major result of this study indicate that inhibition of voltage-gated TTX sensitive or resistant sodium channels in DRG neurons likely contributes to analgesic/anti-hyperalgesia effects of orphenadrine.

2. Methods

2.1 Mutagenesis and expression of recombinant sodium channels

Full-length cDNA encoding wild-type (WT) hNav1.4 (skeletal muscle isoform), hNav1.5 (cardiac isoform), and hNav1.1 (central and peripheral neuron isoform) channels

were subcloned in the mammalian expression vector pRc-CMV or pCMV-Script [5,31,48] and hNav1.7 (peripheral neuron isoform) was subcloned in a modified pcDNA3/pBR222 expression vector [23].

The F1586C mutation of hNav1.4 was engineered by standard two-step PCR-based site-directed mutagenesis. All PCR reactions were performed using P*fu* DNA polymerase (Stratagene, La Jolla, CA) for high-fidelity amplification. The complete coding region of channel mutant cDNA was sequenced to exclude any polymerase errors.

Transient expression of WT hNav1.5 and hNav1.7 in HEK293 cells was achieved by 10-µg plasmid transfection using the calcium phosphate coprecipitation method [12]. These channels were co-transfected with the gene reporter CD8 in a 10:1 plasmid mass ratio. Cells identified with microbeads coated with anti-CD8 antibody (Dynal, Norway) were used for patch-clamp experiments 36-96 hours after transfection. Permanent expression of WT hNav1.1, WT hNav1.4 as well as F1586C mutant was achieved in HEK293 cells by the same transfection method followed by clone selection with geneticin (GIBCO-Invitrogen, Italy).

2.2 primary cultures of sensory neurons

Dissociation of DRG neurons from 5-6 week-old, male Wistar rats was performed as previously described [7]. Briefly, the rats were deeply anesthetized with halothane and sacrificed by cutting the carotid arteries in accordance with the Guide for the Care and Use of Laboratory Animals and institutional guidelines. Excised thoraco-lumbar DRG were incubated for 45 min. in Hank's balanced salt solution (HBSS) supplemented with 2 mg/ml of collagenase Type IA (Sigma) at 37°C. After incubation, the DRG were rinsed several time with HBSS and gently triturated through the smoothed tip of Pasteur pipettes. Neurons were cultured in Dulbecco's modified Eagle's medium (DMEM) supplemented with 10% heat-inactivated fetal calf serum, 50 U/ml penicillin-streptomycin, 2 mM L-glutamine, 25 mM glucose, 25 ng/ml nerve growth factor (Invitrogen) and 2 ng/ml glial-derived neurotrophic factor (Invitrogen). Neurons were incubated in a humidified atmosphere (5 % CO_2, 37°C) for 14-20 hours before recording.

2.2 Voltage-clamp studies

Whole-cell sodium currents (I_{Na}) were recorded at room temperature (20-22°C) using Axopatch 1D or 200B amplifiers (Axon Instruments, Union City, CA, USA). Voltage clamp protocols and data acquisition were performed with pCLAMP software (version 6.0, 9.2, or 10.0, Axon Instruments) through a 12-bit A-D/D-A interface (Digidata 1200 or 1344, Axon Instruments). Patch pipettes had resistance ranging from 1 to 3 MΩ. Currents were low-pass filtered at 2 kHz (-3 dB) by the four pole Bessel filter of the amplifier and digitized at 10-20 kHz.

For recordings in HEK293 cells, after rupturing the patch membrane, a 25 ms-long test pulse to -30 mV from a holding potential (HP) of -120 mV was applied to the cell at a low frequency until stabilization of I_{Na} amplitude and kinetics was achieved (typically 5 minutes) [12]. Data were considered for analysis only from cells exhibiting series resistance errors <5 mV. Little (<5%) or no rundown was observed within the experiments. Specific voltage protocols and analysis procedures are described in the Results section.

In DRG neurons, TTX-resistant sodium currents were recorded using specific voltages allowing separation of high voltage-activated (HVA) currents (known as SNS or PN3) and low voltage-activated (LVA) currents (known as NaN or SNS2). With TTX and La^{3+} in the bath solution, the HVA current is mainly supported by Nav1.8 sodium channels, whereas the LVA current results mainly from activation of Nav1.9 sodium channels

[7,8,33]. The HVA current was elicited from a holding potential of –55 mV to a test pulse of –10 mV. At this HP, the Nav1.9 channels are mostly inactivated. At 0.1 and 2 Hz stimulation frequencies, the leak and capacitive currents were subtracted online using the P/4 protocol of pClamp software. At 10 Hz stimulation frequency, subtraction was performed offline using an adequately scaled current response to hyperpolarizing stimulation. The LVA current was elicited from an HP of –100 mV to –60 mV at 0.1 Hz stimulation frequency. At – 60 mV, the Nav1.8 channels are closed, allowing activation of solely Nav1.9 channels. The use of fluoride in the pipette solution increases amplitude and negatively shifts the voltage dependence of LVA currents. A P/6 protocol was used for leak and capacitive current subtraction.

2.3 Drugs and solutions

All reagents as well as hydrochloride salts of mexiletine and orphenadrine were purchased from Sigma-Aldrich (Milan, Italy), except differently indicated. For patch-clamp recordings of heterologously expressed sodium channels, the pipette solution contained in mM 120 CsF, 10 CsCl, 10 NaCl, 5 EGTA and 5 Hepes, and the pH was set to 7.2 with CsOH, while the bath solution contained in mM 150 NaCl, 4 KCl, 2 $CaCl_2$, 1 $MgCl_2$, 5 Hepes and 5 glucose. The pH was set to 7.4 with NaOH. For patch-clamp recordings in DRG sensory neurons, the pipette solution contained in mM 100 CsCl, 30 CsF, 8 NaCl, 2.4 $CaCl_2$, 1 $MgCl_2$, 5 EGTA, 10 Hepes, 4 ATP, and 0.4 GTP, and the pH was set to 7.3 with NaOH. The bath solution contained in mM 131 NaCl, 3 KCl, 2.5 $CaCl_2$, 1 $MgCl_2$, 10 Hepes, 10 glucose, 0.5 tetrodotoxin (TTX), and 5 La^{3+}. The pH was set to 7.35 with NaOH.

Orphenadrine was diluted in bath solution at desired concentration and the pH was adjusted to 7.4. The patched HEK293 cell was continuously exposed to a stream of control or drug-supplemented bath solution flowing out from a plastic capillary. During recordings, the DRG neurons were perfused with bath solution at a flow rate of 3 ml/min. The bath solution was recycled to limit sparing of TTX. Both perfusion systems allowed application of drug in less than 1 min.

2.4 Statistical analysis

Average data are presented as means ± S.E.M. and statistical difference between the means was evaluated using Student's unpaired or paired *t*-test, with $P < 0.05$ considered as significant.

3. Results

3.1 Dose- and frequency-dependent block of four sodium channel subtypes by orphenadrine

We tested orphenadrine on four sodium channel subtypes encoded by different genes. While the hNav1.4 channel (SCN4A gene) is expressed exclusively in skeletal muscle, the hNav1.5 channel (SCN5A gene) is the main cardiac isoform and is expressed also in some areas of the central nervous system as well as in immature or denervated skeletal muscle, the hNav1.1 channel (SCN1A gene) is expressed in central and peripheral neurons and cardiac myocytes, and the hNav1.7 channel (SCN9A) is predominantly expressed in peripheral neurons, including the DRG where it is concentrated in small C fiber nociceptors [4]. Wild-type hNav1.1, hNav1.4, hNav1.5, and hNav1.7 channels were transiently or permanently expressed in HEK293 cells, and the resulting I_{Na} were recorded with patch-clamp technique in the whole-cell configuration [12].

Externally applied orphenadrine produced both tonic and use-dependent block of I_{Na} elicited by depolarizing pulses to -30 mV from an holding potential (HP) -120 mV. Tonic block was assayed 3 min after drug application by measuring the reduction of I_{Na} elicited at 0.1 Hz, whereas use-dependent block was further obtained by increasing stimulation frequency to 10 Hz. Applying this protocol in the absence of drug produced no significant change in I_{Na} amplitude (not shown). Figure 1A shows representative examples of hNav1.4 current traces recorded before (control) and after application of 30 µM orphenadrine. The drug reduced the amplitude of peak I_{Na} by 24 ± 6 % at 0.1 Hz and 81± 5 % at 10 Hz (n=4). Figure 1B shows representative examples of hNav1.7 current traces recorded in the presence of 100 µM orphenadrine. The drug reduced the amplitude of peak I_{Na} by 48 ± 4 % at 0.1 Hz and 82 ± 4 % at 10 Hz (n=4). The inhibitory effect of orphenadrine was dose-dependent. The concentration-response curves were fitted with the first-order binding function,

$$I_{DRUG}/I_{CONTROL} = 1/\{1+([drug]/ IC_{50})^{nH}\} \quad (1)$$

where IC_{50} (µM) is the half-maximum inhibitory concentration and nH is the slope factor (Fig. 1C and D). The values of IC_{50} and nH are reported in Table 1. Little or no difference was found between the four sodium channel isoforms. Compared to the effects of the well-known sodium channel blockers, mexiletine and flecainide, on hNav1.4 in the same experimental conditions, orphenadrine was equipotent to flecainide and more potent than mexiletine at 0.1 Hz, while its IC_{50} at 10 Hz was about 3-fold smaller than that of the two other drugs indicating a high frequency-dependent profile [12,13]. The block of orphenadrine of sodium channel was completely reversible (see below).

3.2 State-dependent binding affinities of orphenadrine to hNa1.4 channels

According to the modulated receptor hypothesis, use-dependent block can be explained from different binding affinities to the closed and open/inactivated channels [20]. For similar reason, the block of I_{Na} at the HP of -120 mV probably reflects the combination of binding to both the resting and inactivated sodium channels at this HP [12,50]. We calculated the drug-binding affinities to resting (K_R) and inactivated (K_I) sodium channels using hNav1.4 to allow direct comparison with data previously obtained with mexiletine and flecainide. To evaluate K_R, we first measured tonic block of the channels while maintaining the cell hyperpolarized at -180 mV for 120 s (prepulse) and, only after that, the cell was depolarized at 0.1 Hz frequency (Fig. 2A, B). At the HP of -180 mV, the entire population of the channels are in the closed state, ready to open in response to the first pulse depolarization. No change in I_{Na} occurred in absence of drug. In presence of drug, a reduction of I_{Na} amplitude, labeled tonic block (TB), was observed on the first pulse after the 120 s-long prepulse, which reflects binding to closed channels. Little or no additional block was observed at 0.1 Hz. At 10 Hz, a huge use-dependent block developed, which was reversed on turning back to 0.1 Hz stimulation. Finally, TB can be fully reversed by washing out the drug. We calculated the K_R as the IC_{50} value of concentration-response curves for TB occurring during the prepulse (Fig. 2C). The calculated K_R for orphenadrine was 161 ± 23 µM. For comparison, the K_R values for mexiletine and flecainide on hNav1.4 channels were 800 µM and 480 µM, respectively [12,13]. Thus orphenadrine binds to resting sodium channels with relatively high affinity.

Because inactivated channels are non-conducting, calculation of affinity constant for inactivated channels can be only indirect. We calculated the TB at HP= -90 mV using the same protocol as in Fig. 2A, except a 35 ms-long hyperpolarized pulse at -180 mV was introduced before the test-pulse at -30 mV to allow inactivated at -90 mV channel to recover from inactivation, thereby assuring that the reduction of I_{Na} was attributable only to closure of drug-bound channels (Fig. 3A). In these conditions, the IC_{50} value for TB was

23.6 ± 3.4 µM (K_{APP} in equation 2). Using the Bean's equation derived from the modulated receptor hypothesis,

$$K_I = (1-h)\cdot(1/K_{APP} - h/K_R)^{-1} \quad (2)$$

where K_{APP} is the apparent affinity constant at the potential considered and the terms h and (1-h) are the proportions of closed and inactivated channels at this potential as determined from steady-state inactivation curves (Fig. 3B) [2]. With h = 0.9197 at -90 mV, the calculated K_I value was 2.2 µM. Compared to mexiletine (K_I = 6 µM) and flecainide (K_I = 18 µM) on hNav1.4 channels, orphenadrine appeared as a potent blocker of sodium channels inactivated from the closed state [13].

3.3 Orphenadrine binds to the local anesthetic receptor

Sodium channel block characteristics suggest that orphenadrine may bind to the local anesthetic receptor within the channel pore. In particular, the aromatic moiety and the charged amine of LAs were proposed to interact with two aromatic residues of the segment 6 of domain IV (Phe1764 and Tyr1771 in the rat Nav1.2 channel) through hydrophobic and π-cation interactions [39]. The phenylalanine residue appeared as the more important amino acid for inactivated channel block. This amino acid is conserved in the various mammalian voltage dependent sodium channel subtypes (Fig. 4A). We engineered the corresponding F1586C mutation into the hNav1.4 template. The mutant express well in HEK cells and clones with permanent expression were obtained. Similarly to F1764A in Nav1.2, the F1586C mutation in hNav1.4 positively shifted the voltage-dependence of channel availability by 7.9 mV (Table 1). The local anesthetic mexiletine was first tested on the F1586C mutant to verify whether this amino acid is critical for LA binding in hNav1.4 channels (Fig 4B and D). The IC_{50} values for block of F1586C channels by mexiletine were 1340 µM at 0.1 Hz and 1089 µM at 10 Hz, compared to IC50 values of 235 µM at 0.1 Hz and 37 µM at 10 Hz for blocking wild-type (WT) hNav1.4 channels in similar conditions [12]. Thus mexiletine was 6-fold (0.1 Hz) and 29-fold (10 Hz) less potent in blocking F1586C mutants than WT channels. Consequently the IC_{50} value for F1586C blockade at 0.1 Hz was greater than the K_R of mexiletine for WT channels (~800 µM, see ref. [12]), and the use-dependence was almost zeroed by the mutation, confirming that the phenylalanine residue in position 1586 is critical for binding of LAs to inactivated channels. Importantly, the effects of orphenadrine on F1586C recapitulated those of mexiletine (Fig. 4C and E). At 0.1 Hz, 100 µM orphenadrine was needed on F1586C currents to obtain an effect similar to 30 µM on WT channels. The concentration-effect relationships of orphenadrine on F1586C sodium currents indicated a IC_{50} value of 206 ± 10 µM at 0.1 Hz and 127 ± 14 µM at 10 Hz, which are about two- and ten-fold greater than those measured for WT channels. As for mexiletine, the IC_{50} value for F1586C blockade was greater than the K_R for WT channels, and very little use-dependent block was observed on F1586C currents.

3.4 Use-dependent block of hNav1.7 channels by clinical dose of orphenadrine

The serum concentrations of orphenadrine used clinically for analgesia are in the range of 0.1-0.4 µg/mL, corresponding to 0.03-0.13 µM [26]. Thus we tested the effects of 0.1 µM orphenadrine on hNav1.7 channels using various stimulation frequency and a holding potential of -90 mV (Fig. 5). At this HP, significant use-dependent reduction of sodium currents was observed in absence of drug at 5 and 10 Hz frequencies. However, the reduction of sodium currents was significantly accentuated in presence of the low drug concentration. Steady-state reduction of peak sodium current was significantly greater with

the drug compared to control condition at all the three stimulation frequency tested (Fig. 5D).

3.5 Effects of orphenadrine on TTX-resistant sodium currents in DRG neurons

Other than the tetrodotoxin-sensitive Nav1.7 channel isoform, the tetrodotoxin-resistant Nav1.8 and Nav1.9 subtypes are expressed in DRG neurons and are involved in pain sensation [1,27,33,35,40]. Both these channels have proved very difficult to express in heterologous systems, thus we studied the effects of orphenadrine on TTX-resistant sodium currents in primary cultures of DRG neurons [36]. In sensory neurons, the Nav1.8 channels conduct an HVA sodium current that is the main responsible for action potential rising phase. In contrast the Nav1.9 channel is the molecular correlate of a persistent, LVA sodium current that is potentiated by inflammatory mediators, thereby increasing sensory neuron excitability during peripheral inflammation. Because of their peculiar voltage dependence, the two channels can be distinguished by using specific protocols.

For recording of Nav1.8 currents, we used a depolarized holding potential (-55 mV) that pushes Nav1.9 channel into a slow inactivated state. A depolarized HP also allows to record HVA currents of limited amplitude (1-5 nA) to improve voltage clamp. Representative examples of HVA currents are shown in figure 6. Please note that, as expected for Nav1.8 channels, HVA current activation and inactivation were slower with respect to sodium currents recorded in HEK cells. At 0.1 Hz stimulation, 0.1 µM orphenadrine had a small effect on current amplitude, whereas 1, 10 and 30 µM orphenadrine produced significant reduction (Fig. 6A). The IC_{50} value for inhibition of Nav1.8 channels in these conditions was 6.3 µM (Fig. 6B). We also studied the use-dependent inhibition of Nav1.8 currents by orphenadrine (Fig. 7). In absence of drug, current amplitude is stable at 0.1 Hz stimulation, but is greatly reduced by increasing the stimulation frequency to 2 and 10 Hz. As previously observed in figure 6, using 0.1 Hz stimulation, orphenadrine produced little tonic block at 0.1 µM but huge current inhibition at 10 µM. In addition, use-dependent reduction of sodium currents at 2 and 10 Hz was significantly greater in presence of 0.1 and 10 µM of orphenadrine.

To record LVA currents, we used an holding potential of -100 mV and a test pulse at -60 mV. In the presence of TTX to block TTX-sensitive sodium channels and La^{3+} to block T-type calcium channels, the LVA currents are mainly supported by Nav1.9 channels [7]. The Nav1.9 channels are rather atypical with respect to other sodium channel subtypes, generating little-inactivating, persistent sodium currents at hyperpolarized potentials (Fig. 8). Using fluoride as the main intracellular anion, amplitude of the LVA current increased dramatically within 3-5 minutes after patch membrane rupture [8,34]. However, current amplitude ran down soon after, reaching a more stable low amplitude level, as shown in Figure 8A. When applied on the maximally-activated Nav1.9 current, orphenadrine (10 µM) reduced current amplitude by 29.4 % (Fig. 8B). The drug effect was partly reversed upon washout, while currents were entering the run-down process. When applied on the residual current after run-down, orphenadrine reversibly decreased Nav1.9 currents by 28.7 % (Fig. 8C). In average, the inhibition of Nav1.9 currents by 10 µM orphenadrine was 28.5 ± 0.9 % (n= 5).

4. Discussion

Orphenadrine is a drug acting on multiple targets, including histaminic, muscarinic, and NMDA receptors, as well as the noradrenaline reuptake system, although it shows lower affinity with respect to known specific ligands [24,37,41,46]. It was introduced into the market as a medication for Parkinson's disease, providing control of symptoms when

used as monotherapy, but its psychotoxic, cognitive and autonomic adverse events may limit its use in some patients [29]. Randomized trials have also demonstrated muscle relaxing properties of orphenadrine without impairment of normal muscle tone or voluntary movements [6]. Orphenadrine is also used as analgesic either alone or in combination with paracetamol/acetaminophen [21]. The antinociceptive effect of orphenadrine was investigated in mice, suggesting that the drug may reduce different types of nociceptive transmission. In humans, orphenadrine proved benefits with respect to placebo against shoulder, neck, and low back pain, as well as acute and chronic painful musculoskeletal conditions [21]. More recently, orphenadrine was able to exert an analgesic/anti-hyperalgesic effect in a human model of capsaicin-dependent inflammatory pain [42]. The exact molecular mechanism by which orphenadrine induces analgesia is still unknown. It is possible that antihistaminergic properties and NMDA-receptor inhibition may play a role for the observed analgesic effects. Our results strongly support the inhibition of voltage-gated sodium channels as a contributor to analgesic action of orphenadrine.

We demonstrate that orphenadrine blocks voltage-gated sodium channels with a mechanism analogous to a local anesthetic: effect is concentration, voltage, and frequency-dependent. Moreover, the F1586C mutation, located at a position putatively involved in LA binding, greatly reduces I_{Na} inhibition by orphenadrine and zeroes use-dependence, as it does for mexiletine. This result indicates that the phenylalanine is important for the binding of orphenadrine to inactivated sodium channels. The molecule of orphenadrine has a chemical structure similar to sodium channel blockers, like the local anesthetic lidocaine, the antiarhythmic mexiletine, and the anticonvulsant phenytoin, which consists of an aromatic hydrophobic tail linked to a hydrophilic tertiary amine group by ester chain. Its pKa (9.05 ± 0.01) and Log P (3.78 ± 0.01) values indicate that neutral form is highly lipophilic, while the charged form predominates at physiological pH (percentage of ionization is 97.8 % at pH 7.4, as calculated with Handerson-Hasselbach equation). Voltage- and use-dependent block are related to different affinities for closed and inactivated channels. The K_R for orphenadrine is about 5-fold and 3-fold lower compared to those of mexiletine and flecainide, while the K_I is 3-fold and 9-fold reduced, respectively [12,13]. These results indicate that orphenadrine is a potent blocker of closed and inactivated sodium channels. On one hand, the superior lipophilia of orphenadrine may favor access of the drug to closed channels; on the other hand, the diphenyl structure would strengthen drug-channel interactions at the binding site, especially to the inactivated channel. Indeed, It has been found that other diphenyl compounds have a binding affinity to the inactivated sodium channels ~100-fold higher than to the resting channels [25].

The use-dependence block of sodium channels may contribute to the clinical efficacy of orphenadrine as analgesic compound. Indeed, it has been hypothesized for many years that voltage-gated sodium channels might play specialized roles in nociception and pain mechanisms [10]. It is clear from animal studied that Nav1.7, Nav1.8 and Nav1.9 all play important roles in inflammatory and neuropathic pain. Voltage-gated sodium channels in sensory neurons have been implicated in several chronic painful neuropathies that arise from peripheral nerve injury [27,40]. Human studies have shown that Nav1.7 is crucial for experiencing physiological pain sensations since gain-of-function mutations in the *SCN9A* gene encoding this channel subtype can result in severe chronic pain sensations [15]. Many types of pain appear to reflect neuronal hyperexcitability, so the use-dependent block of sodium channel is thought to be effective in the treatment of chronic pain [14]. We observed a significant use-dependent block of hNav1.7 channels at the hp of -90 mV with the clinically-relevant 0.1 μM concentration of orphenadrine, suggesting that clinical doses may produce a very significant block of high-frequency action potential firing in depolarized, physiologic or pathologic conditions. We also demonstrated that low doses of orphenadrine blocks tetrodotoxin-resistant sodium channels in DRG sensory neurons,

which are conducted by Nav1.8 and Nav1.9 channel subtypes. Because orphenadrine blocks both tetrodotoxin-sensitive (Nav1.1, Nav1.4, Nav1.7) and tetrodotoxin-resistant (Nav1.5; Nav1.8, Nav1.9) channel subtypes, it is quite probable that the block of the entire cohort of sodium channels expressed in sensory neurons may contribute to its analgesic action.

On the other hand, blood concentrations of orphenadrine greater than 0.5 µg/mL (~0.2 µM) may cause toxic reactions [28]. Such toxic effects are frequently observed because orphenadrine is widely available and the drug can be deliberately abused for its analgesic, stimulating, and euphoriant effects, as well as for suicide purpose [18,38]. Besides anticholinergic side effects, orphenadrine can produce both central and peripheral adverse reactions, including generalized tonic-clonic seizures and life-threatening arrhythmias [11,16]. Low dose of orphenadrine was also shown to precipitate long QT and Torsades-de-Pointes tachycardia in a patient with congenital long QT syndrome [32]. Recent studies suggest that cardiac and neuronal toxicity may be linked to the action of orphenadrine on HERG channels, which contribute to the action potential repolarization phase in the heart and to spike-frequency accommodation in the nervous system [43,47]. Our results show that orphenadrine inhibits the sodium channel subtypes expressed in heart and central neurons. Although sodium channel blockers may be used as antiarrhythmics and anticonvulsants for their use-dependent mechanism of action, exaggerated inhibition of sodium currents by high orphenadrine doses would induce proarrhythmic and proconvulsive effects, especially because the drug displays a relatively high affinity to resting channels.

In conclusion, our study shows that orphenadrine blocks different subtypes of voltage-gated sodium channels at clinically relevant doses, including the Nav1.7, Nav1.8 and Nav1.9 channel subtypes that are primarily involved in nociception. These results indicate a new mechanism likely contributing to its analgesic effect. On the other hand, the inhibition of sodium channels in various tissues may be a source for toxic reactions.

5. Acknowledgements

We are grateful to prof. Enzo Wanke (Milan) for the gift of hNav1.7 plasmid. We thank Dr. Claudio Bruno (Bari) for measurement of orphenadrine Log P and pKa, and Jizhe Hao (Marseille) for help with primary culture of DRG neurons. This study was supported by Telethon-Italy (grant GGP04140 to D.C.C.). The authors declare no conflict of interest.

6. References

[1] Akopian AN, Souslova V, England S, Okuse K, Ogata N, Ure J, Smith A, Kerr BJ, McMahon SB, Boyce S. The tetrodotoxin-resistant sodium channel SNS has a specialized function in pain pathways. Nat Neuroscience 1999;2:541-548.
[2] Bean BP, Cohen CJ, Tsien RW. Lidocaine block of cardiac sodium channels. J Gen Physiol 1983;81:613-642.
[3] Black JA, Liu S, Tanaka M, Cummins TR, Waxman SG. Changes in the expression of tetrodotoxin-sensitive sodium channels within dorsal root ganglia neurons in inflammatory pain. Pain 2004;108:237-247.
[4] Catterall WA, Perez-Reyes E, Snutch TP, Striessnig J. International Union of Pharmacology XLVIII. Nomenclature and structure-function relationships of voltage-gated calcium channels. Pharmacol Rev 2005;57:411-425.
[5] Chahine M, Bennett PB, George AL Jr, Horn R. Functional expression and properties of the human skeletal muscle sodium channel. Pflügers Arch 1994;427:136-142.

[6] Chou R, Peterson K, Helfand M. Comparative efficacy and safety of skeletal muscle relaxants for spasticity and musculoskeletal conditions: a systematic review. J Pain Symptom Manage 2004;28:140-175.
[7] Coste B, Crest M, Delmas P. Pharmacological dissection and distribution of NaN/Nav1.9, T-type Ca^{2+} currents, and mechanically activated cation currents in different populations of DRG neurons. J Gen Physiol 2007;129:57-77.
[8] Coste B, Osorio F, Padilla F, Crest M, Delmas P. Gating and modulation of presumptive NaV1.9 channels in enteric and spinal sensory neurons. Mol Cell Neurosci 2004;26:123-134.
[9] Cox JJ, Reimann F, Nicholas AK. An SCN9A channelopathy causes congenital inability to experience pain. Nature 2006;444:894-898.
[10] Cummins TR, Sheets PL, Waxman SG. The roles of sodium channels in nociception: Implications for mechanisms of pain. Pain 2007;131:243-257.
[11] Danze LK, Langdorf MI. Reversal of orphenadrine-induced ventricular tachycardia with physostigmine. J Emerg Med 1991;9:453-457.
[12] Desaphy J-F, De Luca A, Tortorella P, De Vito D, George AL Jr, Conte Camerino D. Gating of myotonic Na channel mutants defines the response to mexiletine and a potent derivative. Neurology 2001;57:1849-1857.
[13] Desaphy J-F, De Luca A, Didonna MP, George AL Jr, Conte Camerino D. Different flecainide sensitivity of hNav1.4 channels and myotonic mutants explained by state-dependent block. J Physiol 2004;554:321-334.
[14] Devor M, Wall PD, Catalan N. Systemic lidocaine silences ectopic neuroma and DRG discharge without blocking nerve conduction. Pain 1992;48:261-268.
[15] Drenth JP, Waxman SG. Mutations in sodium-channel gene SCN9A cause a spectrum of human genetic pain disorders. J Clin Invest 2007;117:3603-9.
[16] Elmalem J, Garnier R, Nguyen Huu Chieu R, Bismuth C, Efthymiou ML. Acute poisoning by orphenadrine. Ann Med Interne (Paris) 1985,136:640-645.
[17] Fernández-Sánchez MT, Díaz-Trelles R, Groppetti A, Manfredi B, Brini AT, Biella G, Sotgiu ML, Novelli A. Nefopam, an analogue of orphenadrine, protects against both NMDA receptor-dependent and independent veratridine-induced neurotoxicity. Amino Acids 2002;23:31-36.
[18] Gjerden P, Engelstad KS, Pettersen G, Slordal L. Fatalities caused by anticholinergic antiparkinsonian drugs. Analysis of findings in a 11-year national material. Tidsskr Nor Laegeforen 1998;118:42-44. Norwegian
[19] Gold RH, Treatment of low back syndrome with oral orphenadrine citrate. Curr Ther Res 1978;23:271-276.
[20] Hille B. Local anesthetic: hydrophilic and hydrophobic pathways for the drug receptor reaction. J Gen Physiol 1977;69:497-515.
[21] Hunskaar S, Donnell D. Clinical and pharmacological review of the efficacy of orphenadrine and its combination with paracetamol in painful conditions. J Int Med Res 1991;19:71-87.
[22] Kim YS, Shin YK, Lee C, Song J. Block of sodium currents in rat dorsal root ganglion neurons by diphenhydramine. Brain Res 2000;881:190-198.
[23] Klugbauer N, Lacinova L, Flockerzi V, Hofmann F. Structure and functional expression of a new member of the tetrodotoxin-sensitive voltage-activated sodium channel family from human neuroendocrine cells. EMBO J 1995;14:1084-1090
[24] Kornhuber J, Parsons CG, Hartmann S, Kamolz S, Thome J, Riederer P. Orphenadrine is an uncompetitive N-methyl-D-aspartate (NMDA) receptor antagonist: binding and patch clamp studies. J Neural Trans Gen Sect 1995;2:237-246.

[25] Kuo CC, Huang RC, Luo BS. Inhibition of Na^+ current by diphenhydramine and other diphenyl compounds: molecular determinants of selective binding to the inactivated channels. Mol Pharmacol 2000;57:135-143.
[26] Labout JJM, Thijssen CT, Keijser GGJ, Hespe W. Difference between single and multiple dose pharmacokinetics of orphenadrine hydrochloride in man. Eur J Clin Pharmacol 1982;21:343-350.
[27] Lai J, Hunter JC, Porreca F. The role of voltage-gated sodium channels in neuropathic pain. Curr Opin Neurobiol 2003;13:291-297.
[28] Lee SY, Oh HJ, Kim JW, Kim YG, Moon CJ, Lee EH. Pharmacokinetic study of orphenadrine using high-performance liquid chromatography-tandem mass spectrometry (HPLC-MS/MS). J Chromatogr B Analyt Technol Biomed Life Sci 2006;839:118-123.
[29] Lees A. Alternatives to levodopa in the initial treatment of early Parkinson's disease Drugs Aging 2005;22:731-740.
[30] Legroux-Crespel E, Sassolas B, Guillet G, Kupfer I, Drupe D, Misery L. Treatment of familial erythermalgia with the association of lidocaine and mexiletine. Ann Dermatol Venereol 2003;130:429-433.
[31] Lossin C, Wang DW, Rhodes TH, Vanoye CG, George AL Jr. Molecular basis of an inherited epilepsy. Neuron 2002;34:877-884.
[32] Luzza F, Raffa S, Saporito F, Oreto G. Torsades de pointes in congenital long QT syndrome following low-dose orphenadrine. Int J Clin Pract 2006;60:606-608.
[33] Maingret F, Coste B, Padilla F, Clerc N, Crest M, Korogod SM, Delmas P. Inflammatory mediators increase Nav1.9 current and excitability in nociceptors through a coincident detection mechanism. J Gen Physiol 2008;131(3):211-25.
[34] Maruyama H, Nakamoto M, Matsunomi T, Zheng T, Nakata Y, Wood JN, Ogata N. 2004. Electrophysiological characterization of the tetrodotoxin-resistant Na+ channel, Nav(1.9), in mouse dorsal root ganglion neurons. Pflugers Arch. 2004;449:76-87.
[35] Priest BT, Murphy BA, Lindia JA, Diaz C, Abbadie C, Ritter AM, Liberator P, Iyer LM, Kash SF, Kohler MG, Kaczorowski GJ, MacIntyre DE, Martin WJ. Contribution of the tetrodotoxin-resistant voltage-gated sodium channel Nav1.9 to sensory transmission and nociceptive behavior. Proc Natl Acad Sci USA 2005;102:9382-9387.
[36] Priest BT, Kaczorowski GJ. Blocking sodium channels to treat neuropathic pain. Exp Opin Ther Targets 2007;11:291-306.
[37] Pubill D, Canudas AM, Pallàs M, Sureda FX, Escubedo E, Camins A, Camarasa J. Assessment of the adrenergic effects of orphenadrine in rat vas deferens. J Pharm Pharmacol 1999;51:307-312.
[38] Pullen GP, Best NR, Maguire J. Anticholinergic drug abuse: a common problem? Br Med J 1984;289:612-613.
[39] Ragsdale DS, McPhee JC, Scheuer T, Catterall WA. Molecular determinants of state-dependent block of Na channels by local anesthetic. Science 1994;265:1724-1728.
[40] Roza C, Laird JM, Souslova V, Wood JN, Cervero F. The tetrodotoxin-resistant Na+ channel Nav1.8 is essential for the expression of spontaneous activity in damaged sensory axons of mice. J Physiol 2003;550:921-926.
[41] Rumore MM, Schlichting DA. Analgesic effects of antihistaminics. Life Sci 1985;36:403-416.
[42] Schaffler K, Reitmeir P. Analgesic effects of low-dose intravenous orphenadrine in the state of capsaicin hyperalgesia. A randomised, placebo-controlled, double-blind cross-over study using laser somatosensory evoked potentials obtained from capsaicin-irritated skin in healthy volunteers. Arzneimittelforschung 2004;54:673-679.
[43] Scholz EP, Konrad MF, Weiss DL, Zitron E, Kiesecker C, Bloehs R, Kulzer M, Thomas D, Kathofer S, Bauer A, Maurer MH, Seemann G, Katus HA, Karle CA. Anticholinergic antiparkinson drug orphenadrine inhibits HERG channels: block attenuation

by mutations of the pore residues Y652 or F656. Naunyn-Schmiedeberg's Arch Pharmacol 2007;376:275-284.
[44] Standaert DG, Young AB. Treatment of central nervous system degenerative disorders. In Goodman and Gilman's the Pharmacological Basis of Therapeutics, 9th edn, Hardman JG, Limbird LE, Molinoff PB, Ruddon RW, Goodman Gilman A (Eds), McGraw-Hill, New York, 1995,503-519.
[45] Sweeney PJ. Parkinson's disease: managing symptoms and preserving function. Geriatrics 1995;509:24-31.
[46] Syvälahti EK, Kunelius R, Laurén L. Effects of antiparkinsonian drugs on muscarinic receptor binding in rat brain, heart and lung. Pharmacol Toxicol 1988;62:90-94.
[47] Taglialatela M, Timmerman H, Annunziato L. Cardiotoxic potential and CNS effects of first-generation antihistamines. Trends Pharmacol Sci 2000;21:52-6.
[48] Wang DW, George AL Jr, Bennett PB. Comparison of heterologously expressed human cardiac and skeletal muscle sodium channels. Biophys J 1996;70:238-245.
[49] Waxman SG. Nav1.7, its mutations, and the syndromes that they cause. Neurology 2007;69:505-507.
[50] Wright SN, Wang SY, Kallen RG, Wang GK. Differences in steady-state inactivation between Na channel isoforms affect local anesthetic binding affinity. Biophys J 1997;73:779-788.

Table 1. IC_{50} values for orphenadrine block of four human voltage-gated sodium channel isoforms and the F1586C hNav1.4 mutant.

	IC_{50} at 0.1 Hz (μM)	nH at 0.1 Hz	IC_{50} at 10 Hz (μM)	nH at 10 Hz	$V_{1/2}$ (mV)
hNav1.4	92.9 ± 12.0	1.3 ± 0.2	13.2 ± 1.1	1.5 ± 0.2	-72.3 ± 0.2 (17)
hNav1.5	70.4 ± 6.1	1.2 ± 0.1	13.0 ± 1.2	1.3 ± 0.2	-79.7 ± 0.7 (17)
hNav1.1	110.3 ± 10.2	1.3 ± 0.1	12.9 ± 2.1	1.2 ± 0.2	-71.0 ± 0.2 (18)
hNav1.7	92.1 ± 9.1	1.2 ± 0.1	17.2 ± 1.9	1.1 ± 0.1	-62.1 ± 0.7 (20)
F1586C	206 ± 10	1.4 ± 0.1	127 ± 14	1.2 ± 0.2	-64.4 ± 0.2 (24)

The half-maximum inhibitory concentration (IC_{50}) and the slope factor (nH) values were calculated using equation (1) at the HP of -120 mV from the concentration/response relationships shown in Fig. 1 and 4. The half-maximum inactivation potential ($V_{1/2}$) was calculated from the fit with Boltzmann equation of steady-state inactivation relationships obtained as in Fig. 3B using the cells (number indicated within brackets) used for determination of IC_{50} value.

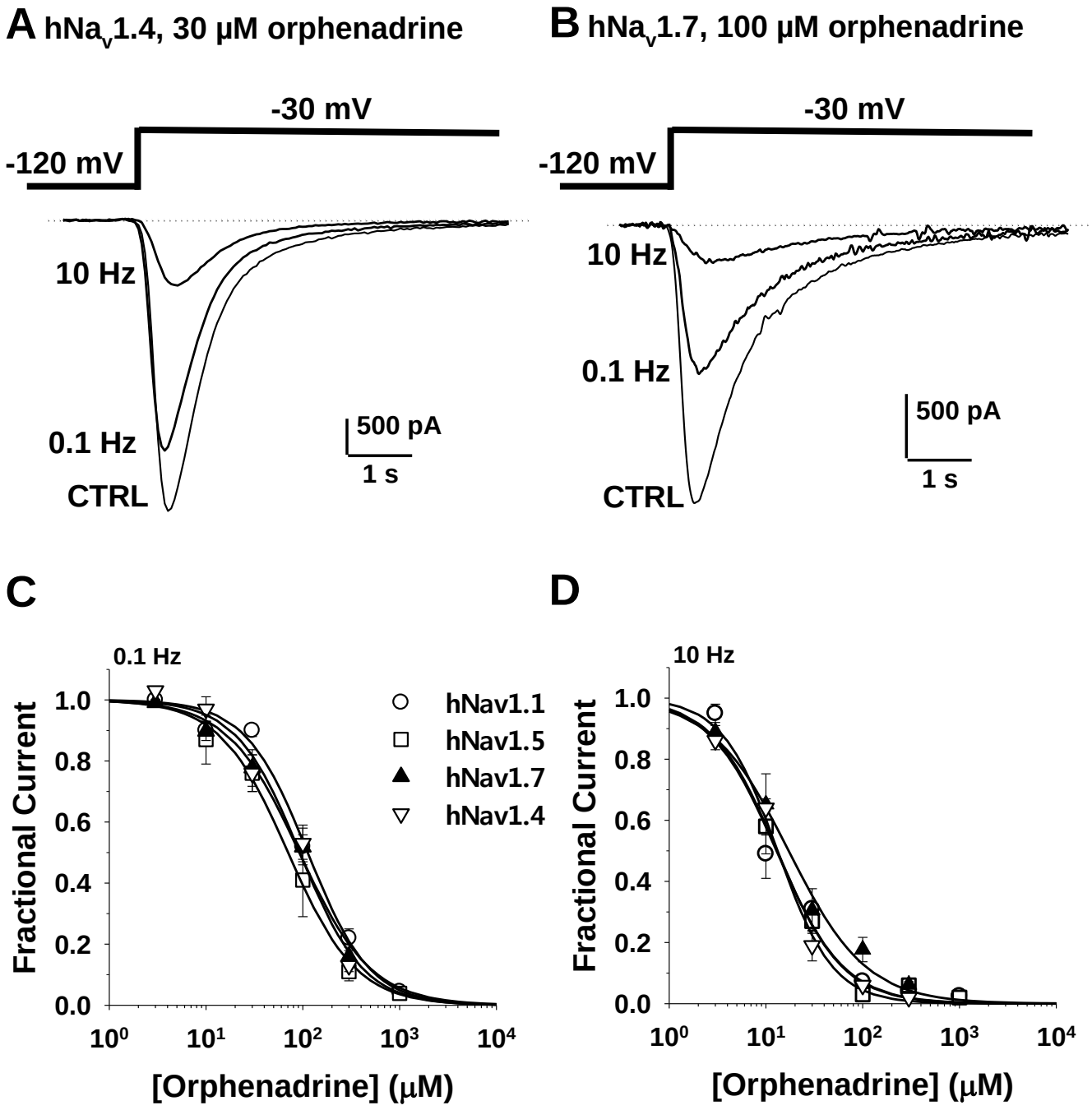

Fig. 1. Dose-dependent and use-dependent block of four sodium channel subtypes by orphenadrine. The block of sodium currents by orphenadrine was assessed 3 min after drug application by measuring the reduction of I_{Na} elicited with a 25 ms-long test pulse from −120 mV to −30 mV at stimulation frequencies of 0.1 and 10 Hz. **A**, Effects of 30 µM orphenadrine on hNav1.4 currents **B**, Effects of 100 µM orphenadrine on hNav1.7 currents. The concentration-response curves for orphenadrine block were constructed at 0.1 (**C**) and 10 Hz (**D**) and fitted with equation (1). Each data point is the mean ± S.E.M. of at least 3 cells. The calculated IC_{50} and nH values ± S.E. of the fit are reported in Table 1.

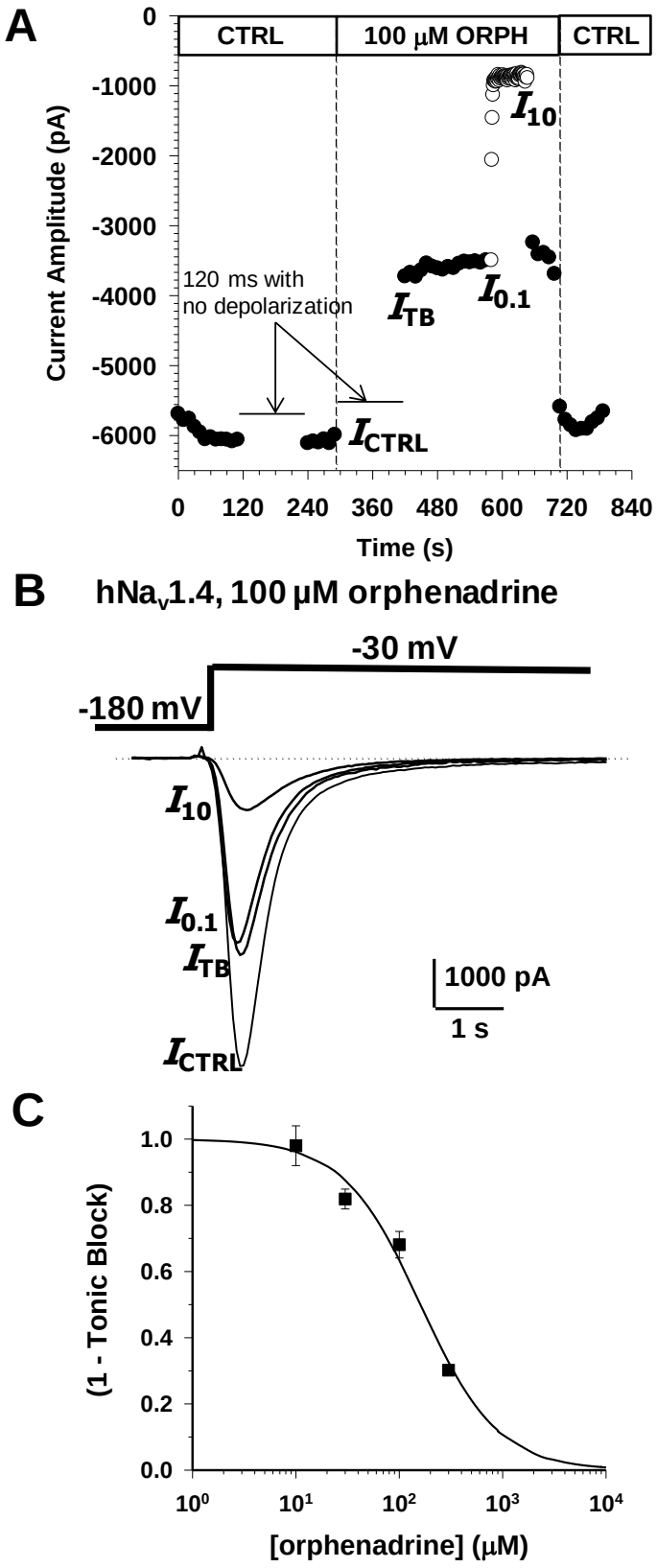

Fig. 2. Affinity of orphenadrine for resting, closed hNav1.4 channels. **A**, time course of peak I_{Na} in a HEK293 cell expressing hNav1.4 channels. The cell was held at the HP of −180 mV and depolarized for 25 ms to −30 mV at 0.1 Hz (plain circles) and 10 Hz (open circles), except in correspondence to arrows where the HP was maintained with no depolarization. Tonic block was measured in presence of 100 μM orphenadrine at the first pulse depolarization. Little or no block was observed at 0.1 Hz, whereas a huge use-dependent block was observed at 10 Hz. **B**, traces of hNav1.4 I_{Na} measured at the times reported in A: I_{CTRL} was measured just before application of the drug, I_{TB} correspond to tonic block, $I_{0.1}$ corresponds to the steady-state block reached at 0.1 Hz, and I_{10} corresponds to the steady-state block at 10 Hz. C, concentration-response curve was constructed for tonic block (I_{TB}/I_{CTRL}) of hNav1.4 I_{Na} currents measured as in A. Each data point is the mean ± S.E.M. of at least 3 cells. The relationship was fitted with equation (1), where the calculated IC_{50} corresponds to affinity to resting, closed channels K_R. The K_R value ± S.E. of the fit was 161 ± 23 μM. The calculated slope factor nH ± S.E. of the fit was 1.2 ± 0.2.

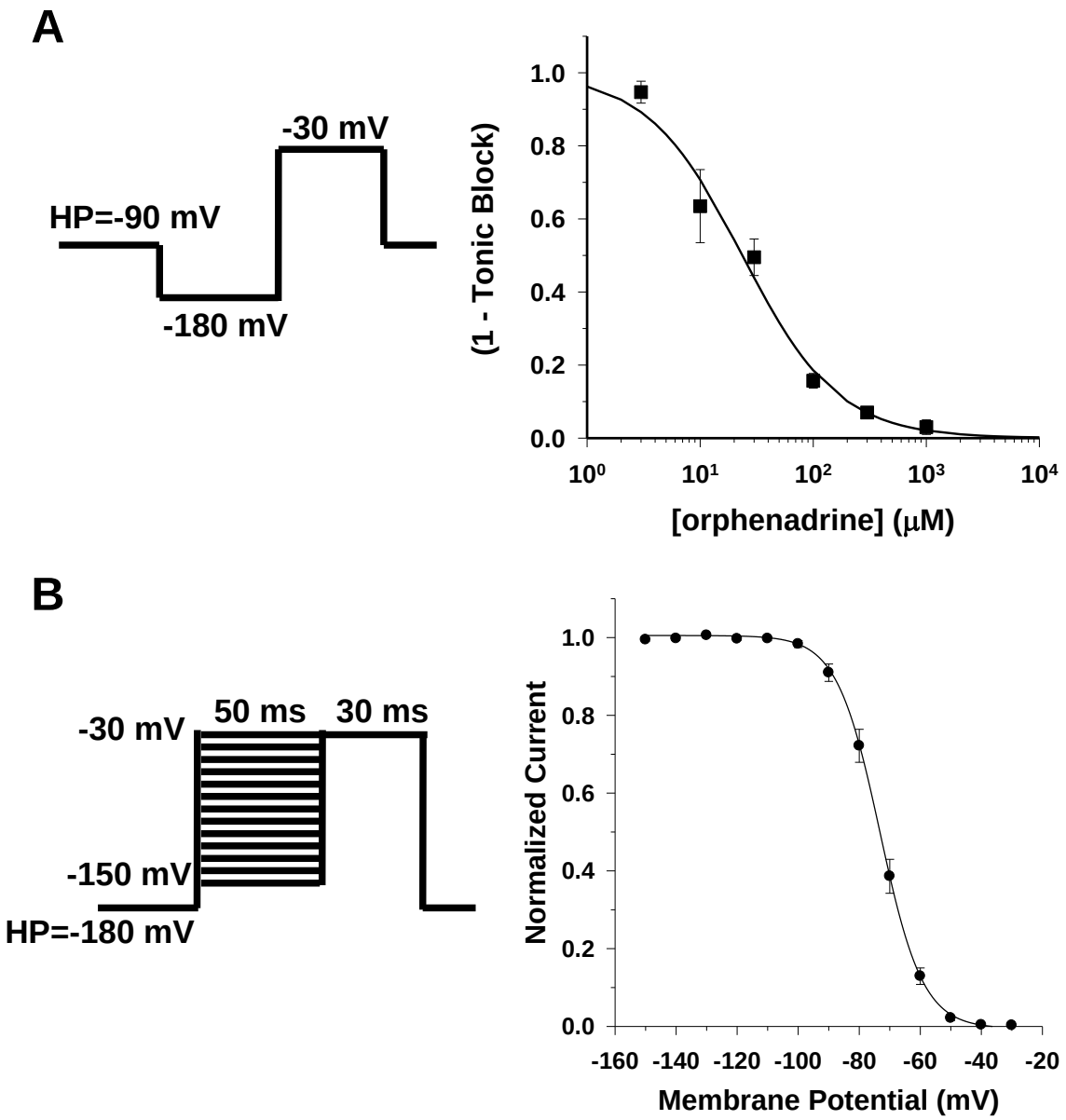

Fig. 3. Affinity of orphenadrine for inactivated hNav1.4 channels. **A**, concentration-response curve was constructed for I_{TB}/I_{CTRL} measured as in Figure 2A, except the HP was -90 mV and a 35 ms-long hyperpolarized pulse at -180 mV was introduced before the test-pulse at -30 mV to allow inactivated at -90 mV channel to recover from inactivation, thereby assuring that the reduction of I_{Na} was attributable only to closure of drug-bound channels. Each data point is the mean ± S.E.M. of at least 3 cells. The relationship was fitted with equation (1), where the calculated IC_{50} value corresponds to apparent affinity constant (K_{APP}). The K_{APP} value ± S.E. of the fit was 23.6 ± 3.4 μM. The calculated slope factor nH ± S.E. of the fit was 1.0 ± 0.1. **B**, steady-state inactivation curve of I_{Na} in a HEK293 cell expressing hNav1.4. INa was evoked by a 20 ms-long test pulse to − 30 mV after a 50 ms-long conditioning pulse to potentials ranging from −150 to −30 mV in 10-mV increments; the HP was −180 mV. The peak I_{Na} recorded during the test pulse was plotted against the conditioning pulse potential. The relationship was fitted with the Boltzmann equation, $I_{Na}/I_{Na,max} = 1/\{1+\exp[(V - V_{1/2})/S]\}$, where $V_{1/2}$ (mV) is the half-maximum inactivation potential and S (mV) is the slope factor. Each data point is the mean ± S.E.M. of the 18 cells used for determination of K_{APP}. The $V_{1/2}$ value ± S.E. of the fit was -73.2 ± 0.1 mV. The calculated slope factor S ± S.E. of the fit was -7.0 ± 0.1 mV. From this relationship, the proportions of closed (h) and inactivated (1 - h) channels was determined at -90 mV and inserted together with K_R and K_{APP} values into equation (2) to calculate the affinity for inactivated channel (K_I), which was 2.2 μM.

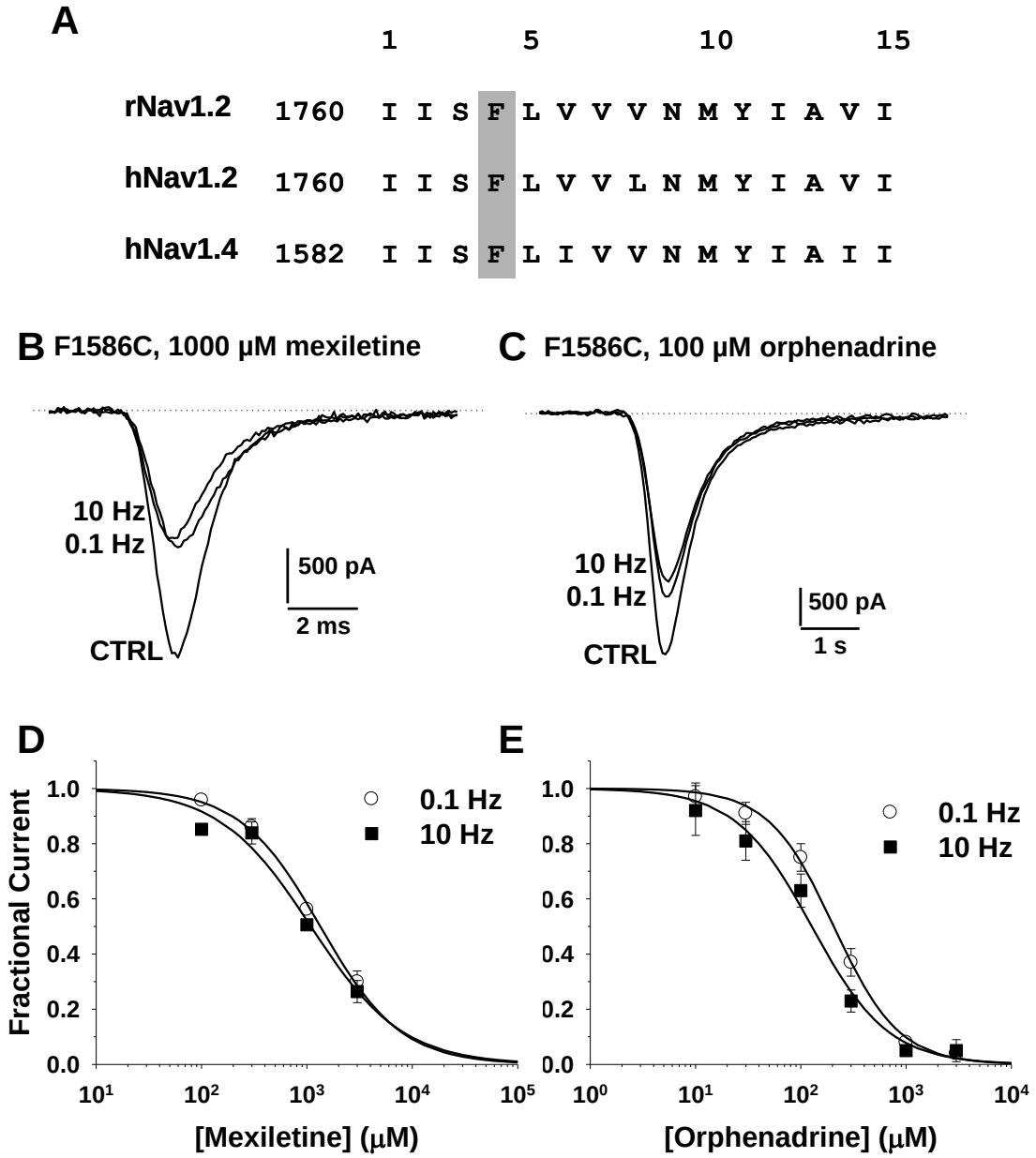

Fig. 4. Binding of orphenadrine and mexiletine to the local anesthetic receptor. **A**, Alignment of aminoacidic sequence within the 6th segment of domain IV of the α sodium channel subunit of rat neuronal (rNav1.2), human neuronal (hNav1.2), and human skeletal muscle (hNav1.4) channels. The phenylalanine residue, originally found in rNav1.2 to be critical for binding of local anesthetics, is conserved among sodium channel subtypes and among species. The corresponding F1586C mutation was introduced into the hNav1.4 template. **B and C**, Representative traces of I_{Na} recorded in HEK293 cells expressing the F1586C hNav1.4 channel. Mexiletine and orphenadrine block was assessed 3 min after drug application by measuring the reduction of I_{Na} elicited with a 25 ms-long test pulse from −120 mV to −30 mV at stimulation frequencies of 0.1 and 10 Hz. **D and E**, concentration-response curves for mexiletine and orphenadrine block were constructed at 0.1 and 10 Hz using the protocol described above and fitted with equation (1). Each data point is the mean ± S.E:M. of at least 3 cells. For mexiletine, the calculated IC_{50} values ± S.E. of the fit were 1340 ± 72 µM at 0.1 Hz and 1089 ± 181 µM at 10 Hz. The calculated slope factor nH ± S.E. of the fit were 1.1 ± 0.1 at 0.1 Hz and 1.0 ± 0.2 at 10 Hz. For orphenadrine, the calculated IC_{50} and nH values are reported in Table 1.

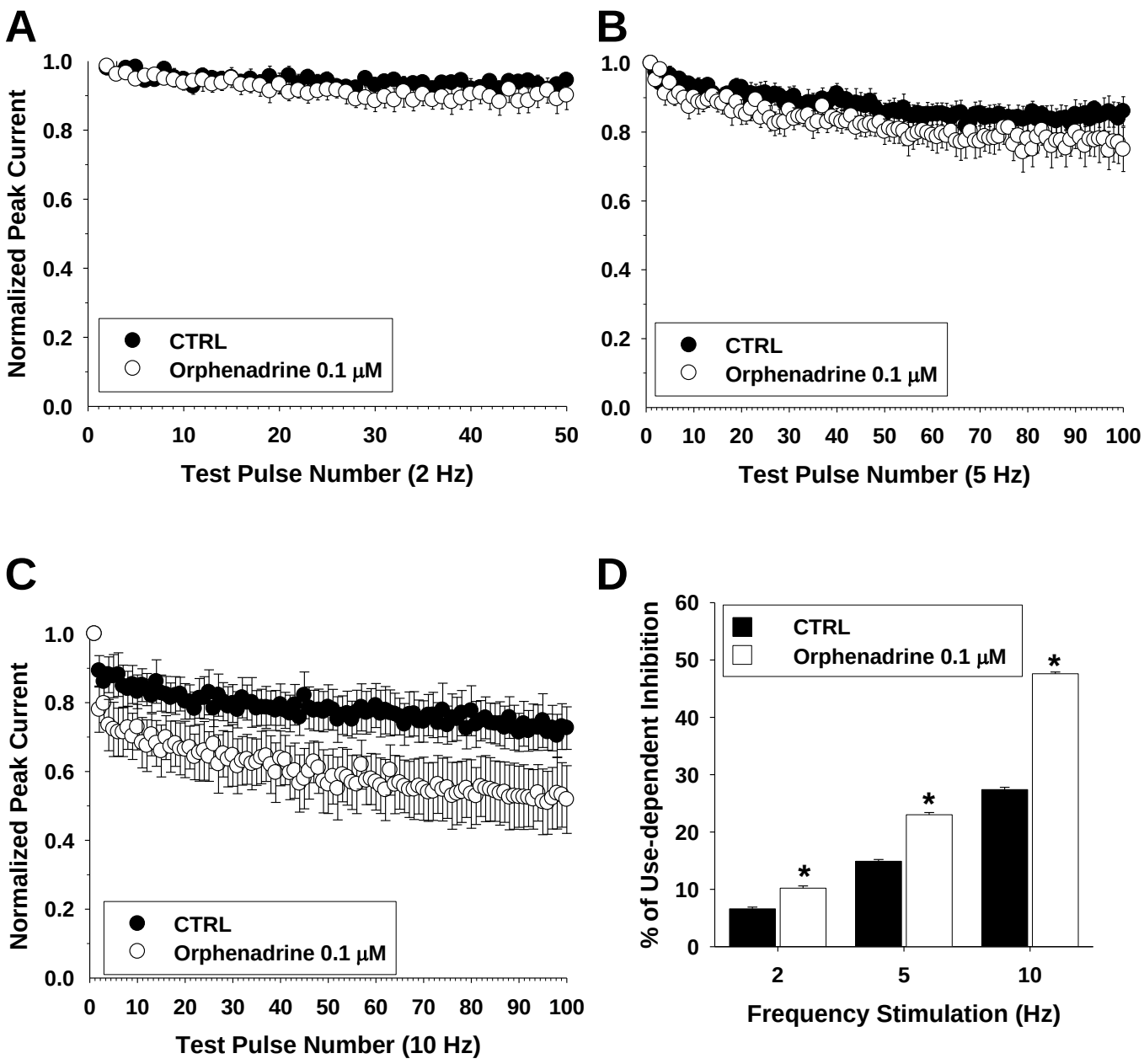

Fig. 5. Use-dependent block of hNav1.7 channels by the clinically-relevant 0.1 μM concentration of orphenadrine. **A, B, and C**, Sodium currents were elicited with a 12 ms-long test pulse at -30 mV from the holding potential of -90 mV at 2, 5, or 10 Hz in control conditions (CTRL) then in presence of 0.1 μM orphenadrine. The peak current amplitude was normalized with respect to the first test-pulse peak current amplitude and plotted against the test-pulse number. Each point is the mean ± S.E.M. from 5 cells. **D**, The last ten amplitude values (pulse number 41 to 50 at 2 Hz and 91 to 100 at 5 and 10 Hz) were averaged to calculate the percentage of use-dependent inhibition at steady state. Paired Student's *t*-test indicated significant differences (at least $P<0.01$) between CTRL and drug at the three stimulation frequencies tested.

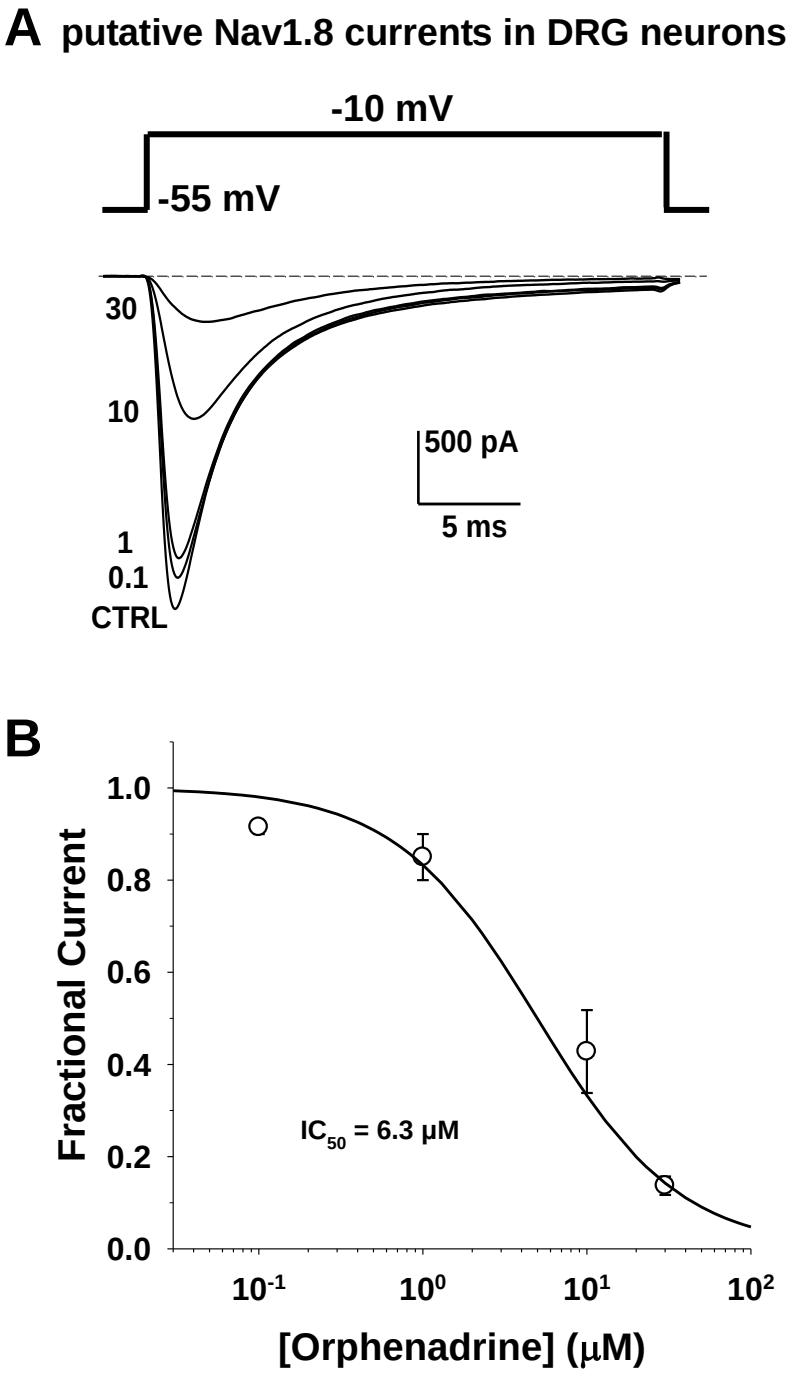

Fig. 6. Tonic block of Nav1.8 channels by orphenadrine in rat DRG sensory neurons. **A**, High-voltage activated (HVA) currents were recorded in primary culture of rat DRG neurons with whole-cell patch-clamp technique by depolarizing the cell to -10 mV for 25 ms from an holding potential of -55 mV every 10 s (frequency stimulation of 0.1 Hz). With tetrodotoxin in the bath solution, the HVA currents are supported mainly by the Nav1.8 sodium channel subtype. Current traces were recorded in a representative neuron before (CTRL) and after successive application of 0.1, 1, 10, and 30 µM orphenadrine. **B**, concentration-response curve for tonic block of Nav1.8 channels by orphenadrine was constructed at 0.1 Hz using the protocol described in A and fitted with equation (1). Each data point is the mean ± S.E.M. from at least 3 DRG neurons. The calculated IC_{50} values ± S.E. of the fit were 6.3 ± 1.4 µM and the slope factor nH was 0.97 ± 0.19.

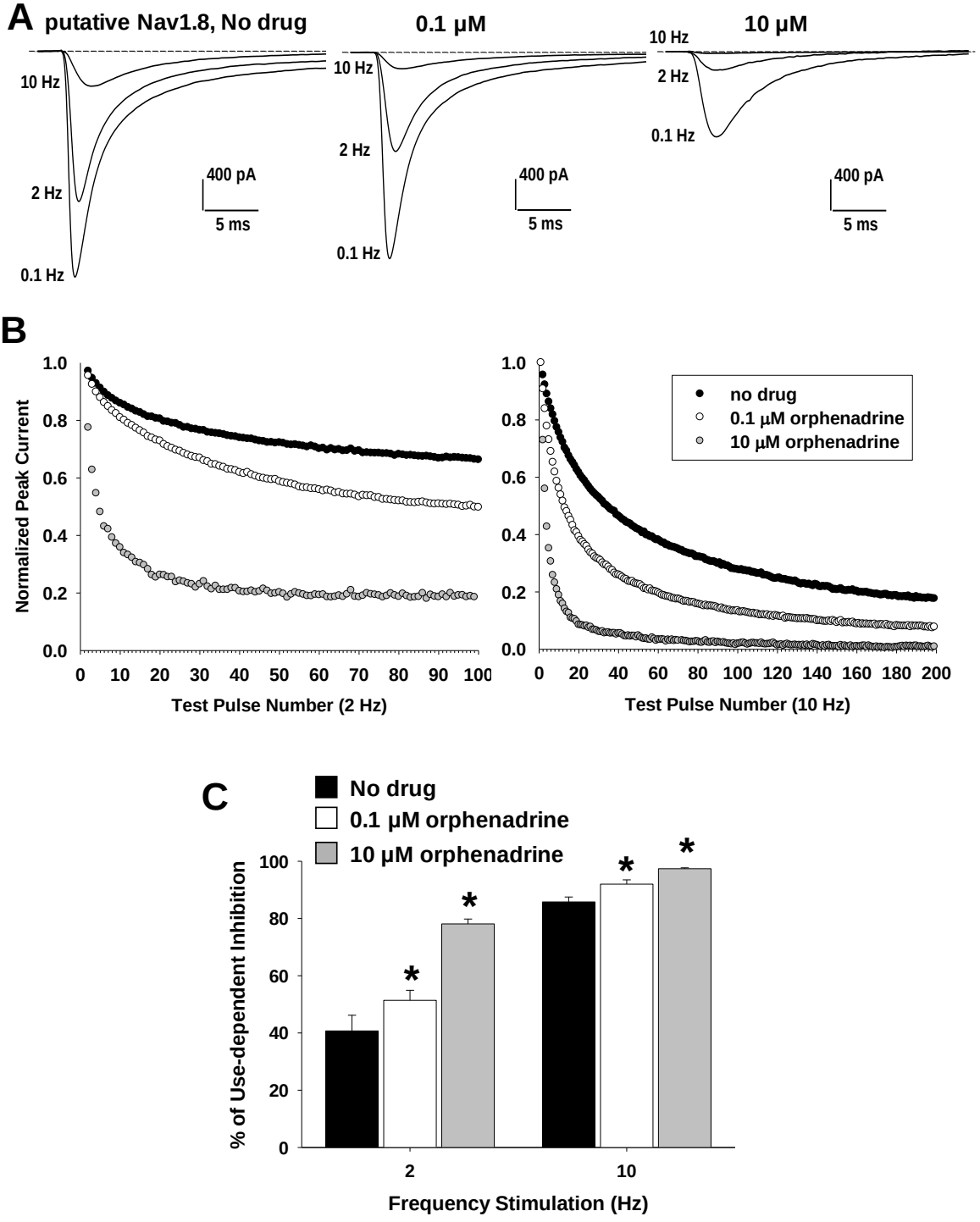

Fig. 7. Use-dependent block of Nav1.8 channels by orphenadrine in rat DRG sensory neurons. **A**, HVA sodium currents were recorded in a representative rat DRG neuron as in figure 6 using 0.1, 2, and 10 Hz stimulation frequency before and after successive applications of 0.1 and 10 μM orphenadrine. **B**, time course of use-dependent reduction of Nav1.8 currents in the same neuron as in A at 2 (left) and 10 (right) Hz stimulation frequency before and after successive applications of 0.1 and 10 μM orphenadrine. **C**, Mean ± S.E.M. percentage of use-dependent Nav1.8 current reduction measured in 4 DRG neurons before and after successive applications of 0.1 and 10 μM orphenadrine. The symbol * indicates significant difference (at least $P<0.05$) with respect to control condition (no drug) calculated with paired Student's *t*-test.

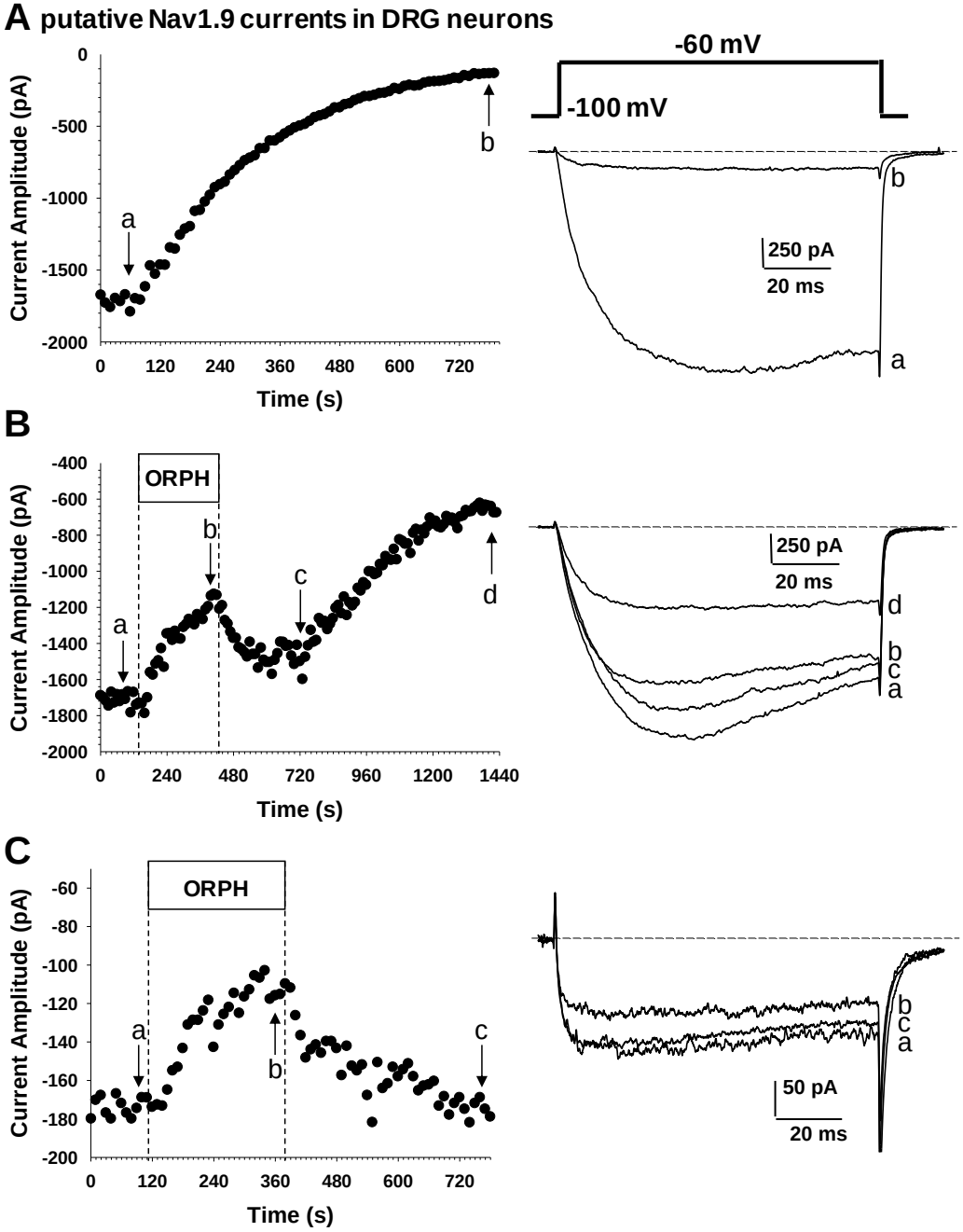

Fig. 8. Effects of orphenadrine on Nav1.9 channels in rat DRG sensory neurons. A, low-voltage activated (LVA) currents were recorded in primary culture of rat DRG neurons with whole-cell patch-clamp technique by depolarizing the cell to -60 mV for 100 ms from an holding potential of -100 mV every 10 s (frequency stimulation of 0.1 Hz). With tetrodotoxin and La^{3+} in the bath solution, the LVA currents are conducted mainly by the Nav1.9 sodium channel subtype. **A**, Representative time course of the characteristic run-down of Nav1.9 currents recorded with intracellular fluoride in a DRG neuron. Right panel shows current traces extracted at time a (maximum activity) and b (after run-down). **B**, Time course of current amplitude when 10 µM orphenadrine was applied on the maximally-activated Nav1.9 currents in a representative DRG neuron. Right panel shows current traces extracted at time a (maximum Nav1.9 current activation), b (during application of orphenadrine), c (under drug washout), and d (after run-down). **C**, Time course of current amplitude when 10 µM orphenadrine was applied on Nav1.9 currents after run-down in a representative DRG neuron. Right panel shows current traces extracted at time a (after run-down), b (during application of 10 µM orphenadrine), and c (under drug washout).